



Saliva Based Diagnostic Prediction of Oral Squamous Cell Carcinoma using FTIR Spectroscopy

Priya Shree¹ · Yogendra Aggarwal² · Manish Kumar³ · Lakhan Majhee⁴ · Narendra Nath Singh⁵ · Om Prakash⁶ · Akhilesh Chandra⁷ · Simpy Amit Mahuli⁸ · Shoa Shamsi⁸ · Arpita Rai¹

Received: 7 October 2023 / Accepted: 14 October 2023 / Published online: 13 January 2024
© Association of Otolaryngologists of India 2024

Abstract

Oral cancer ranks as the sixth most prevalent form of cancer worldwide, presenting a significant public health concern. According to the World Health Organization (WHO), within a 5-year period following diagnosis, the mortality rate among oral cancer patients of all stages stands at 45%. In this study, a total of 60 patients divided into 2 groups were recruited. Group A included 30 histo-pathologically confirmed OSCC patients and Group B included 30 healthy controls. A standardized procedure was followed to collect saliva samples. FTIR spectroscopy was done for all the saliva samples collected from both Group A and B. An IR Prestige-21 (Shimadzu Corp, Japan) spectrometer was used to record IR spectra in the 40–4000 cm^{-1} range SVM classifier was applied in the classification of disease state from normal subjects using FTIR data. The peaks were identified at wave no 1180 cm^{-1} , 1230 cm^{-1} , 1340 cm^{-1} , 1360 cm^{-1} , 1420 cm^{-1} , 1460 cm^{-1} , 1500 cm^{-1} , 1540 cm^{-1} , 1560 cm^{-1} , and 1637 cm^{-1} . The observed results of SVM demonstrated the accuracy of 91.66% in the classification of Cancer tissues from the normal subjects with sensitivity of 83.33% while specificity and precision of 100.0%. The development of oral cancer leads to noticeable alterations in the secondary structure of proteins. These findings emphasize the promising use of ATR-FTIR platforms in conjunction with machine learning as a reliable, non-invasive, reagent-free, and highly sensitive method for screening and monitoring individuals with oral cancer.

Keywords Oral squamous cell carcinoma · FTIR · Support Vector machine · Vibrational spectroscopic

✉ Arpita Rai
arpita.dirims@gmail.com

Priya Shree
priyashreebds@gmail.com

Yogendra Aggarwal
yaggarwal@bitmesra.ac.in

Manish Kumar
manish@bitmesra.ac.in

Lakhan Majhee
drlakhan35@gmail.com

Narendra Nath Singh
naren_cancer@hotmail.com

Om Prakash
dromprakashomfs@gmail.com

Akhilesh Chandra
drakhilesh_1979@yahoo.com

Simpy Amit Mahuli
dr.simpy@gmail.com

Shoa Shamsi
shamsishoa@gmail.com

- 1 Dental College, Rajendra Institute of Medical Sciences (RIMS), Bariatu, Ranchi, Jharkhand 834009, India
- 2 Department of Bioengineering and Biotechnology, Birla Institute of Technology Mesra, Ranchi, India
- 3 Department of Bioengineering, Birla Institute of Technology, Mesra, Ranchi 835215, India
- 4 Department of Pharmacology, Rajendra Institute of Medical Sciences, Ranchi, India
- 5 Oral Pathology, Microbiology and Forensic Odontology, Dental College, Rajendra Institute of Medical Sciences (RIMS), Bariatu, Ranchi 834009, India
- 6 Oral and Maxillofacial Pathology, Dental College, Rajendra Institute of Medical Sciences (RIMS), Bariatu, Ranchi 834009, India
- 7 Department of Oral Pathology and Microbiology, Faculty of Dental Sciences, Banaras Hindu University, Varanasi, India
- 8 Dental College, Rajendra Institute of Medical Sciences (RIMS), Bariatu, Ranchi 834009, India

Introduction

Oral cancer is the sixth most common cancer in the world and it is one of the major public health problems. Consumption of various tobacco products are associated with higher risk of developing oral cancer compared to persons without any adverse habit. Optimal selection of therapy plays a crucial role in the successful treatment of oral cancer, along with the importance of early diagnosis. The World Health Organization (WHO) has reported a mortality rate of 45% for oral cancer patients across all stages within five years of diagnosis. Notably, individuals with oral squamous cell carcinoma (OSCC) who receive timely treatment exhibit more favourable outcomes, with 80% 5-year survival rates [1]. Enhancing early cancer diagnosis and treatment relies on two key factors: identifying specific biomarkers for cancer detection and developing dependable, user-friendly techniques [2]. Fourier transform infrared (FTIR) spectroscopy emerges as a promising method in this field [3–5]. The vibrational spectroscopic techniques mentioned are characterized by their simplicity, reproducibility, non-destructiveness to tissue, and minimal sample preparation requirements, involving small amounts of material ranging from micrograms to nanograms. Furthermore, these techniques offer valuable molecular-level insights, enabling the study of functional groups, bonding types, and molecular conformations. Spectral bands observed in vibrational spectra are unique to each molecule, providing direct information about its biochemical composition. This method has been previously utilized for detecting and monitoring the treatment of breast cancer [6, 7]. Differences have been shown in the absorption spectra of blood serum from lung cancer patients and healthy individuals [8, 9]. There have been reports in the literature on the diagnosis of cancer of the stomach [10], intestines [11, 12], liver [13], prostate [14, 15], thyroid [16], testicles [17], bladder [18], and other organs [19–22].

Attention is now being focused on saliva as an informative biomaterial for the non-invasive diagnosis and monitoring of the human organism [24, 25]. Saliva is a complex and dynamic biological fluid composed of DNA, RNA, proteins and metabolites. Alterations in the levels of these substances can serve as indicators of systemic diseases or the presence of early-stage oral cancer [9]. The salivary proteome is highly dynamic [10], contains over 3652 proteins and 12,562 peptides, and shares nearly 51% of the proteins and 79% of the plasma peptides [11]. Hence, saliva could be an effective source for screening or monitoring of the malignancy. However, the use of the IR spectroscopy of saliva for oral cancer diagnosis has been limited. In the present work, FTIR spectroscopy of saliva is used to discriminate between OSCC and Healthy control (HC) subjects using support vector machine (SVM).

Material and Method

Study Population

This study was conducted in the Department of Oral Medicine and Radiology, Dental College, RIMS Ranchi. Approval from Internal Research Review Committee and Institutional Ethics Committee were taken before the study protocol was initiated. In this study, a total of 60 patients divided into 2 groups were recruited. Group A included 30 histo-pathologically confirmed OSCC patients and Group B included 30 healthy controls. All patients gave written informed consent to participate in this study.

A detailed demographic data, history of habit of tobacco and alcohol intake and its duration, frequency, quantity were obtained. History of previous malignancies and previous treatments were also obtained along with thorough examination of the head and neck and the soft and hard tissues within the oral cavity for the detection of an OSCC. Adjacent lymphnodes along with cervical lymph nodes for the location, size, mobility, texture, and tenderness were also done by following standard protocol [23].

Saliva Sample Collections

A standardized procedure was followed to collect unstimulated whole saliva samples. The patients were instructed to rinse their mouths with water and refrain from consuming food, drinks, cigarettes, smokeless tobacco, or oral hygiene products for a minimum of one hour before sample collection. The unstimulated whole saliva samples were collected in the morning, specifically between 9 and 10 a.m., while the patient sat comfortably and expectorated saliva into a plastic container as it accumulated in their mouth. Roughly 10 ml of saliva was collected from each patient.

FTIR Spectroscopy Method

FTIR spectroscopy was done for all the saliva samples collected from both Group A and B at Birla Institute of Technology, Ranchi. An IR Prestige-21 (Shimadzu Corp, Japan) spectrometer was used to record IR spectra in the 40–4000 cm^{-1} range.

The samples were thawed and brought to room temperature. One drop of liquid saliva sample was put on sample table by using micropipette and then spectrum was recorded. The spectrum of air was used as a background before each sample analysis. Background and sample spectra were taken at room temperature (around 21–23 °C), at a spectral resolution of 4 cm^{-1} and for each measurement 32 scans were performed. All IR spectra reflecting the dependency of infrared absorbance (abs. units) on the wavenumber were obtained

in no less than 3 consequent tests with 3–5 repetitions each. The original FTIR spectra were normalized and the baseline was corrected using OPUS software.

Spectral Data Processing

All the raw data were transferred into excel sheet and graph was plotted. The spectrum is recorded on a graph with wave-number (cm^{-1}) recorded on X axis and transmittance on Y axis. Absorbance is related to Transmittance as follows $A = \log(1/T)$ where A is absorbance and t is transmittance. Absorbance is linearly proportional to concentration [Beer–Lambert Law] and used for quantitative analysis. Graphs obtained by each group were compiled.

Feature Selection and Data Reduction

FTIR data was also processed with the Kruskal Wallis test along with the principal component analysis (PCA) technique for features selection and data reduction. The Kruskal Wallis test is a non-parametric technique used to test whether the samples originate from the same distribution. Kruskal-Wallis test was used to select significant features based on the median value of two samples and to obtain the p -value of each wave number-variable. If the p value is less than the significance level ($P < 0.05$) for the features it means features with discriminative information are present and those features were selected. PCA is used for statistical analyses of different samples. With PCA the dimensionality of FTIR microscopic imaging datasets is reduced while as much information as possible is retained. The Kruskal Wallis values were selected as features to be used in the SVM classifier.

Support Vector Machine (SVM)

SVM classifier was applied in the classification of disease state from normal subjects using FTIR data. The classifier draws the hyperplane in separating the data points. The total of 60 samples (30 samples of OSCC and 30 samples of healthy control), were divided into training set (80% of data) and test data set (20% of data). The SVM model was

implemented using the Matlab version 2020b using Gaussian kernel. A two-class model was trained to classify the normal and cancer data set. The FTIR data (1000 to 2000 cm^{-1}) were analysed using Kruskal Wallis technique along with PCA as features selected and feature reduction technique, respectively. The PCA used atleast 95% variance in selection of the data. The derived values of true positive (TP), true negative (TN), false positive (FP), and false-negative (FN) have also been used to determine sensitivity, specificity, and accuracy.

$$\text{Sensitivity} = \frac{TP}{TP + FN}$$

$$\text{Specificity} = \frac{TN}{TN + FP}$$

$$\text{Accuracy} = \frac{TP + TN}{TP + TN + FP + FN}$$

Results

Demographic Detail

The OSCC patients in this study ranged from 35 years to 82 years with a mean of 54.13 years ($SD \pm 13.17$). The male: female ratio in OSCC group was 3.2:1. The mean age of healthy control group subject was 24.9years ($SD \pm 5.6$), ranging from 18 to 42 years. In control group, there were 22 males and 8 female (Table 1). Out of 30 OSCC cases, 18 were well differentiated OSCC, 9 were moderately differentiated OSCC and 3 were Poorly differentiated OSCC.

3.2 FTIR Interpretation

Result of FTIR

The peaks were identified at wave no 1180 cm^{-1} , 1230 cm^{-1} , 1340 cm^{-1} , 1360 cm^{-1} , 1420 cm^{-1} , 1460 cm^{-1} , 1500 cm^{-1} , 1540 cm^{-1} , 1560 cm^{-1} , and

Table 1 Showing age wise demographic distribution of the study population

S. No.	Age group (years)	Oral cancer group			Control group		
		Males	Females	Total	Males	Females	Total
1	≤ 40	4	2	6	20	7	27
2	41–50	8	1	9	2	1	3
3	51–60	5	1	6	0	0	0
4	61–70	4	2	9	0	0	0
5	≥ 70	2	1	3	0	0	0
Total		23	7	30	22	08	30

1637 cm^{-1} . It represents the functional group given in Table 2. 1637 cm^{-1} Amide I band of protein and H–O–H deformation of water is the highest peak identified (Fig. 1, Table 2).

Principal Component Analysis

Loading Plot (PCA) demonstrated that the sample 8, 26 and 33 are negatively correlated while others are forming the small angle thus positively correlated (Fig. 2a) and steep scree plot revealed that principal component 1 captured all the information (Fig. 2b). Comparison of principal components to the wave numbers with respect to the Normal and cancerous sample is shown in Fig. 2c

Support Vector Machine Result

The observed results demonstrated the accuracy of 91.66 % in the classification of Cancer tissues from the normal subjects with sensitivity of 83.33% while specificity and precision of 100.0 % (Table 3). The receiver operating characteristic curve presented the area under the curve of 91% (Fig 3).

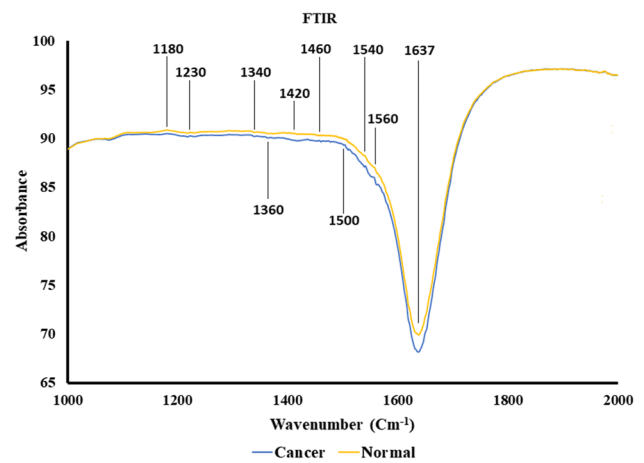


Fig. 1 Showing Graph obtained by compiling OSCC and healthy control group

Discussion

The current study used FTIR spectroscopy combined with machine learning techniques to build discrimination models between the two groups OSCC and Healthy control. FTIR interpretation were performed for 60 saliva samples (30 from oral cancer group and 30 from normal individuals).

Table 2 Assignments of main FTIR peaks, component identification and biomolecules

FTIR bands (cm^{-1})	Band assignment	Component identification	Biomolecules	References
1180		Amide III	Alpha amylase, Albumin, cystains, mucins, proline-rich protein, salivary IgA	Movasaghi 2008 [24], Stuart 2005, [25], Orphanou [26]
1230	PO ₂ —asymmetric stretching (ν asPO ₂ ⁻), (ν C–N)	Nucleic acid (phosphodiester group)/Phospholipid/ Phosphorylated protein, Amide III	Collagen	Bellisola and Sorio 2012 [27]; Orphanou 2015 [26]
1340	ρ w(CH ₂)	Phospholipids, fatty acid, triglyceride, amino acid side chains	Collagen	Movasaghi 2008 [24]
1420	s(COO ₂)	(polysaccharides, pectin)	Glycogen	Rong Wang 2021
1460	CH ₃	CH ₃ of collagen	Collagen	Movasaghi 2008 [24]
1500	Tyrosine ring	Amide II	α -amylase, albumin, cystains, mucins, proline-rich proteins, sIgA	Movasaghi 2008 [24]
1540	δ N–H, ν C–N stretching	Amide II	Tyrosin ring, Alpha amylase, Albumin, cystains, mucins, proline-rich protein, salivary IgA	Stuart 2005 [25]
1560	δ N–H, ν C–N stretching	Amide II	Tyrosin ring, Alpha amylase, Albumin, cystains, mucins, proline-rich protein, salivary IgA	Stuart 2005 [25]
1637	(ν C=O, ν C–N, δ N–H	Amide I	Prolin, Glycine	Movasaghi 2008 [24]; Stuart 2005 [25]

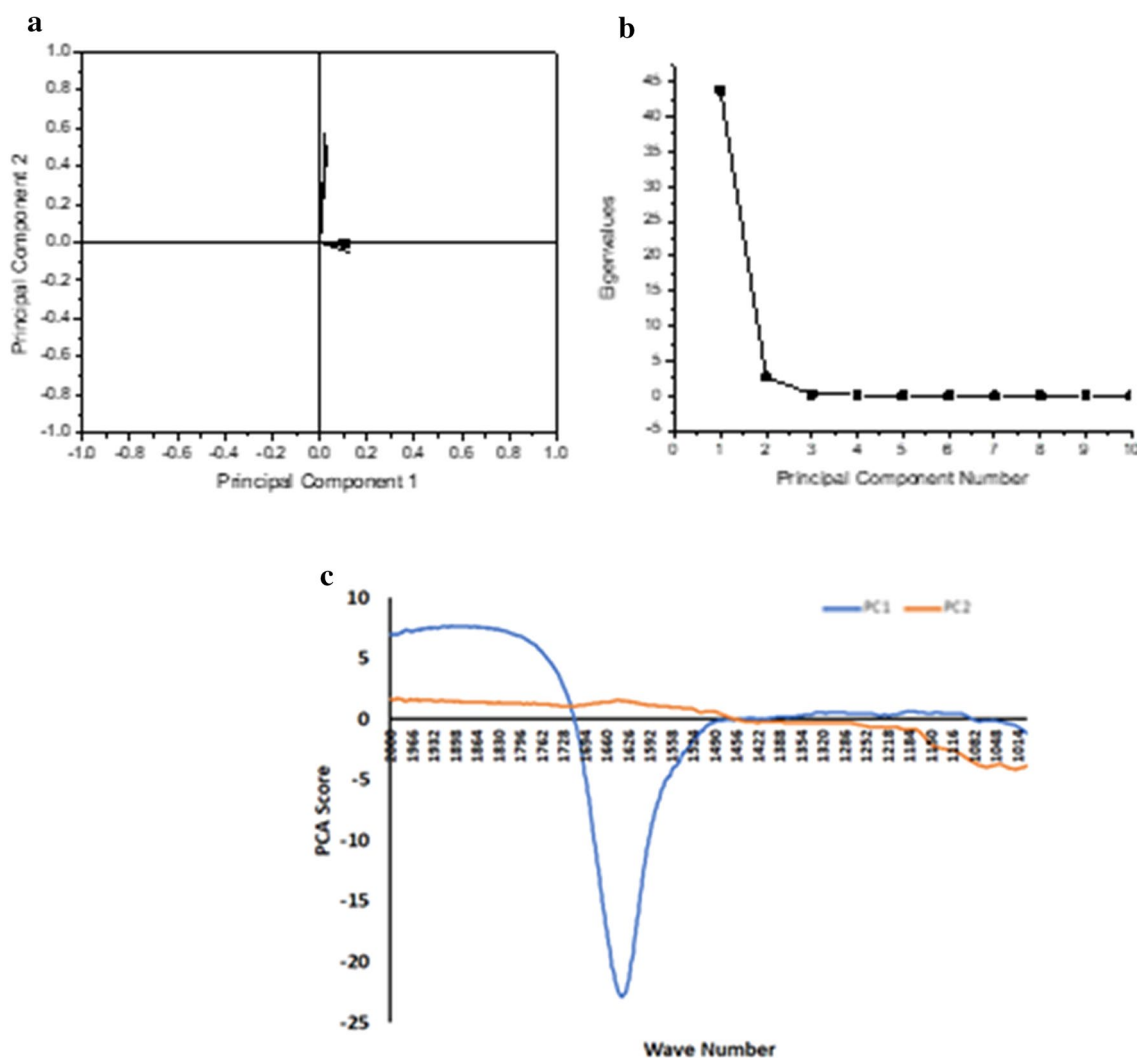


Fig. 2 **a** Loading Plot (PCA). **b** Scree Plot. **c** Comparison of principal components to the wave numbers with respect to the Normal and cancerous sample

Table 3 Support vector machine result

Features (1000 to 2000 wavenumber)				Performance metrics			
Class 1	Class 2	Box Constraint	Kernel Scale	Accuracy (%)	Sensitivity (%)	Specificity (%)	Precision (%)
Cancer	Normal	46.43	0.006	91.66	83.33	100.000	100.000

The peaks obtained were at wave no 1180 cm^{-1} , 1230 cm^{-1} , 1340 cm^{-1} , 1360 cm^{-1} , 1420 cm^{-1} , 1460 cm^{-1} , 1500 cm^{-1} , 1540 cm^{-1} , 1560 cm^{-1} , and 1637 cm^{-1} . Although peaks identified are similar in both the groups, the absorbance of oral cancer group at 1637 cm^{-1} wavenumber was observed to be more than the normal individual group. At 1637 cm^{-1} Amide I band of protein and H–O–H deformation of water is observed. Amides I and II bands are commonly used to investigate the secondary structure of proteins [3]. Example of Secondary Structure of Protein are Prolin and Glycin

[4]. Absorbance is linearly proportional to concentration [Beer–Lambert Law] and used for quantitative analysis. Therefore, it can be interpreted that quantity of anticipated proteins at 1637 cm^{-1} is more in oral cancer group than that of normal individual group.

Wu et al. used fiber-optic ATR spectroscopy on freshly-cut human oral tissues and found that the intensity variation at 1745 cm^{-1} band among normal and malignant tissue. The relative intensities of the 1745 cm bands were strong in the spectra of normal tissues but weak or absent in malignant

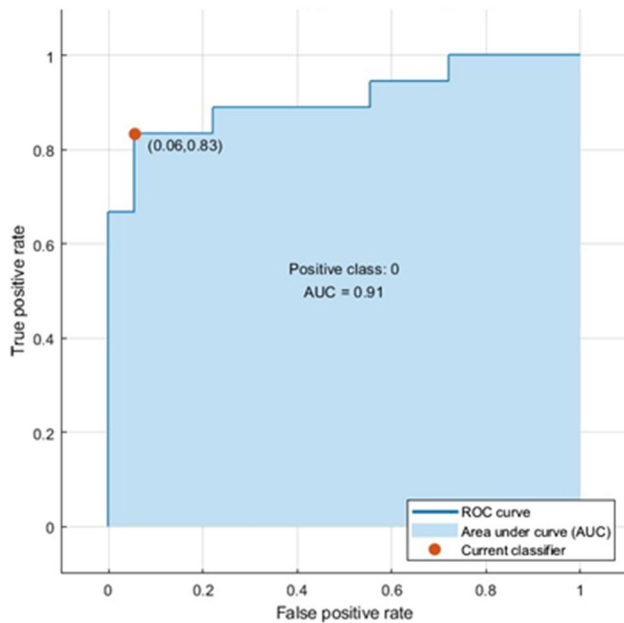


Fig. 3 The receiver operating characteristics of the binary classification of cancer and normal subjects

tissues and the amide I band at 1646 cm^{-1} were good markers for distinguishing normal oral tissue from malignant ones. Whereas in current study showed more distinguishing peak at 1637 cm^{-1} between OSCC and HC group in salivary sample [28].

Shaikh et al. studied on saliva based non-invasive screening of Oral Sub mucous Fibrosis which is a potentially malignant disorder using ATR-FTIR spectroscopy. The researchers noted that the transmission of protein predominantly occurs within the $1300\text{ to }1800\text{ cm}^{-1}$ range. Spectral bands in this region are indicative of the amide II region, likely originating from transmembrane proteins. Moreover, a significant contrast in intensity was observed in the wavenumber range of $900\text{--}1200\text{ cm}^{-1}$. Within this range, the biomolecules primarily exhibit carbohydrate vibrations associated with glucose, fructose, and glycogen. In current study between $900\text{ and }1200\text{ cm}^{-1}$, only one peak 1180 cm^{-1} is observed [29].

Ayelet Zlotogorski-Hurvitz et al. analyzed the Fourier-transform infrared (FTIR) spectra of exosomes found in saliva from patients with oral squamous cell carcinoma (OSCC) and healthy individuals (HI), and evaluates its potential as a diagnostic tool using computational models. The results revealed consistent differences between the IR spectra of OSCC and HI at specific frequencies: 1072 cm^{-1} (indicating nucleic acids), 2924 cm^{-1} and 2854 cm^{-1} (representing membranous lipids), and 1543 cm^{-1} (associated with transmembrane proteins). By employing a PCA-LDA discrimination model, the samples were accurately classified with 100% sensitivity, 89% specificity, and 95%

overall accuracy. Furthermore, the SVM model exhibited a training accuracy of 100% and a cross-validation accuracy of 89%. Notably, the current study found the IR spectrum at 1540 cm^{-1} to be particularly close to the identified characteristics [30].

Banerjee et al. In their study, utilized FTIR spectroscopy to differentiate between oral leukoplakia and histological tissues of oral squamous cell carcinoma (OSCC) using linear and quadratic support vector machine (SVM) with tenfold cross-validation. Through the Feature Forward Selection method, they identified six spectral features (at 1782 , 1713 , 1665 , 1545 , 1409 , and 1161 cm^{-1}) that enabled classification between leukoplakia and OSCC. The classification achieved a sensitivity of 81.3%, specificity of 95.7%, and an overall accuracy of 89.7%. However, in the current study, spectral features at 1540 , 1420 , and 1180 cm^{-1} were found to be different from the identified peaks but closer in proximity [31].

Rai et al. [32] used FTIR spectroscopy together with chemometric techniques to differentiate the serum metabolic signatures of OSMF patients from healthy controls. 19 major peaks ($p < 0.001$) were observed at 1313 , 1544 , 1650 , 1035 , 1169 , 1025 , 1045 , 1151 , 1122 , 1078 , 1725 , 1243 , 1453 , 1398 , 1020 , 1100 , 1039 and 1117 cm^{-1} . By employing multivariate statistical techniques such as PCA, HCA, and PLS-DA, the study successfully achieved a remarkable distinction between spectra of oral submucous fibrosis (OSF) and normal samples. This differentiation was accomplished using nineteen significant wavenumbers ($p \leq 0.001$) ranging from $1725\text{ to }1020\text{ cm}^{-1}$, which correspond to alterations in lipids, proteins, carbohydrates, and nucleic acids. These findings strongly suggest that the combination of FTIR spectroscopy and chemometric analysis holds significant potential in enabling rapid and accurate preoperative screening and diagnosis of OSF [31]. Nearer to these findings in current study 10 peaks between $1180\text{ and }1637\text{ cm}^{-1}$ in saliva sample of OSCC and HC patients. Summarizing all the data obtained from different sources we found some of the FTIR peaks were common in tissue, serum as well as saliva of OSCC or Oral potentially malignant disorders, which can represent the distinguishing biomolecules among both the groups. Hence we can infer that saliva which is the safest biological sample may be used as diagnostic sample in place of serum and tissue for FTIR spectroscopy in diagnosis of OSCC.

Support Vector Machine (SVM) is a classification and regression prediction tool that uses machine learning theory to maximize predictive accuracy while automatically avoiding over-fit to the data. In current study SVM classifier was applied in the classification of disease state from normal subjects using FTIR data. PCA was used assessing the dimensionality of FTIR microscopic imaging datasets. The observed results demonstrated the accuracy of 91.66% in the classification of Cancer tissues from the normal subjects

with sensitivity of 83.33% while specificity and precision of 100.0%.

Banerjee et al. achieved a classification between leukoplakia and OSCC with 81.3% sensitivity, 95.7% specificity, and 89.7% overall accuracy [31]. The SVM showed a training accuracy of 100% and a cross-validation accuracy of 89% between OSCC and Healthy Control (Ayelet Zlotogorski-Hurvitz et al. 2019) [30]. Although the current study contained a rather low number of subjects, the discrimination function model was able to differentiate OSCC from HI salivary sample with accuracy of 91.66%, sensitivity of 83.33% while specificity and precision of 100.0%.

Conclusion

From the research that has been carried out it possible to conclude that salivary samples can be successfully used for ATR-FTIR spectroscopy for distinguishing between healthy individuals and oral cancer patients. We highlighted spectroscopic biomarkers associated with oral cancer development, in particular bands attributed to different proteins and polysaccharide. It has been demonstrated that there are significant changes in secondary structure of proteins upon oral cancer development. These data also highlight the potential of ATR-FTIR platforms coupled with machine learning as a sustainable, reagent-free, non-invasive, and highly sensitive tool for screening and monitoring oral cancer patients. For a comprehensive evaluation, it is essential to have a sufficient sample size in order to ensure accuracy and reliability.

Acknowledgements Authors are thankful to Indian Council of Medical Research, New Delhi, Multi Disciplinary Research Unit, Rajendra Institute of Medical Sciences, Ranchi and Birla Institute of Technology, Mesra, Ranchi

Funding No funding.

Declarations

Conflict of interest The authors have no conflict of interest regarding the publication of this article.

Ethical Approval The study was approved by the Institute Ethics Committee of Rajendra Institute of Medical Sciences, Ranchi (ECR/769/INST/JH/2015/RR-18).

References

- Atkinson AJ Jr, Colburn WA, DeGruttola VB, De Mets DL, Downing GJ, Hoth DF, Oates JA, Peck CC, Schooley RT, Spilker BA, Woodcock J, Zeger SL (2001) Biomarkers and surrogate endpoints: preferred definitions and conceptual framework. *Clin Pharmacol Ther* 69:89–95
- Zubareva GM, Minkin VM, Bordina GY, Belyaeva IA, Lopina NP, Zubarev SM, Kargaplov AV (2009) Infra-red spectrometry in oral liquid study for diagnostic purposes. *Stomatologiia* 88(5):7–10
- Seredin P, Goloshchapov D, Kashkarov V, Ippolitov Y, Bambery K (2016) The investigations of changes in mineral–organic and carbon–phosphate ratios in the mixed saliva by synchrotron infrared spectroscopy. *Results Phys* 6:315–321
- Andrei AB, Fleschin Ş, Aboul-Enein HY (2015) Cancer diagnosis by FT-IR spectrophotometry. *Rev Roum Chim* 60(5–6):415–426
- Elmi F, Movaghar AF, Elmi MM, Alinezhad H, Nikbaksh N (2017) Application of FT-IR spectroscopy on breast cancer serum analysis. *Spectrochim Acta A Mol Biomol Spectrosc* 187:87–91
- Depciuch J, Kaznowska E, Golowski S, Kozirowska A, Zawlik I, Cholewa M, Szmuc K, Cebulski J (2017) Monitoring breast cancer treatment using a Fourier transform infrared spectroscopy-based computational model. *J Pharm Biomed Anal* 143:261–268
- Wang X, Shen X, Sheng D, Chen X, Liu X (2014) FTIR spectroscopic comparison of serum from lung cancer patients and healthy persons. *Spectrochim Acta A Mol Biomol Spectrosc* 122:193–197
- Sun X, Xu Y, Wu J, Zhang Y, Sun K (2013) Detection of lung cancer tissue by attenuated total reflection–Fourier transform infrared spectroscopy—a pilot study of 60 samples. *J Surg Res* 179:33–38
- Sheng D, Wu Y, Wang X, Huang D, Chen X, Liu X (2013) Comparison of serum from gastric cancer patients and from healthy persons using FTIR spectroscopy. *Spectrochim Acta A Mol Biomol Spectrosc* 116:365–369
- Kaznowska E, Depciuch J, Szmuc K, Cebulski J (2017) Use of FTIR spectroscopy and PCA-LDC analysis to identify cancerous lesions within the human colon. *J Pharm Biomed Anal* 134:259–268
- Dong L, Sun XJ, Chao Z, Zhang SY, Zheng JB, Gurung R, Du JK, Shi JS, Zhang YF, Wu JG (2014) Evaluation of FTIR spectroscopy as diagnostic tool for colorectal cancer using spectral analysis. *Spectrochim Acta A Mol Biomol Spectrosc* 122:288–294
- Sheng D, Xu F, Yu Q, Fang T, Xia J, Li S, Wang X (2015) A study of structural differences between liver cancer cells and normal liver cells using FTIR spectroscopy. *J Mol Struct* 1099:18–23
- Baker MJ, Gazi E, Brown MD, Shanks JH, Clarke NW, Gardner P (2009) Investigating FTIR based histopathology for the diagnosis of prostate cancer. *J Biophoton* 2:104–113
- Gazi E, Baker M, Dwyer J, Lockyer NP, Gardner P, Shanks JH, Reeve RS, Hart CA, Clarke NW, Brown MD (2006) A correlation of FTIR spectra derived from prostate cancer biopsies with Gleason grade and tumour stage. *Eur Urol* 50:750–761
- Liu Y, Xu Y, Liu Y, Zhang Y, Wang D, Xiu D, Xu Z, Zhou X, Wu J, Ling X (2011) Detection of cervical metastatic lymph nodes in papillary thyroid carcinoma by Fourier transform infrared spectroscopy. *Brit J Surg* 98:380–384
- Gajjar K, Trevisan J, Owens G, Keating PJ, Wood NJ, Stringfellow HF, MartinHirsch PL, Martin FL (2013) Fourier-transform infrared spectroscopy coupled with a classification machine for the analysis of blood plasma or serum: a novel diagnostic approach for ovarian cancer. *Analyst* 138:3917–3926
- Ollesch J, Heinze M, Heisse HM, Behrens T, Brüning T, Gerwert K (2014) It's in your blood: spectral biomarker candidates for urinary bladder cancer from automated FTIR spectroscopy. *J Biophotonics* 7:216–221
- Zhang XQ, Xu Z, Ling XF, Xu YZ, Wu JG (2010) The application of fourier transform infrared technology in biomedical sphere. *Spectrosc Spect Anal* 30:30–34
- Trevisan J, Angelov PP, Carmichael PL, Scott AD, Martin FL (2012) Extracting biological information with computational analysis of Fourier-transform infrared (FTIR) biospectroscopy datasets: current practices to future perspectives. *Analyst* 137:3202–3215

20. Kelly JG, Singh MN, Stringfellow HF, Walsh MJ, Nicholson JM, Bahrami F, Ashton KM, Pitt MA, MartinHirsch PL, Martin FL (2009) Derivation of a subtype-specific biochemical signature of endometrial carcinoma using synchrotron-based Fourier-transform infrared microspectroscopy. *Cancer Lett* 274:208–217
21. Caetano Júnior PC, Strixino JF, Raniero L (2015) Analysis of saliva by Fourier transform infrared spectroscopy for diagnosis of physiological stress in athletes. *Res Biomed Eng* 31:116–124
22. Rodrigues LM, Magrini TD, Lima CF, Scholz J, da Silva Martinho H, Almeida JD (2017) Effect of smoking cessation in saliva compounds by FTIR spectroscopy. *Spectrochim Acta A Mol Biomol Spectrosc* 174:124–129
23. Bandhakavi S et al (2009) A dynamic range compression and three-dimensional peptide fractionation analysis platform expands proteome coverage and the diagnostic potential of whole saliva. *J Proteome Res* 8(12):5590–5600
24. Movasaghi Z, Rehman S, urRehman DI (2008) Fourier transform infrared (FTIR) spectroscopy of biological tissues. *Appl Spectrosc Rev* 43(2):134–179. <https://doi.org/10.1080/05704920701829043>
25. Stuart BH (2005) Biological applications. In: *Infrared spectroscopy: fundamentals and applications*: John Wiley & Sons Ltd, pp 137–165. ISBN: 9780470011140
26. Orphanou CM (2015) The detection and discrimination of human body fluids using ATR FT-IR spectroscopy. *Forensic Sci Int* 252:e10–e16. <https://doi.org/10.1016/j.forsciint.2015.04.020>
27. Bellisola G, Sorio C (2012) Infrared spectroscopy and microscopy in cancer research and diagnosis. *Am J Cancer Res* 2(1):1
28. Wu J-G, Xu Y-Z, Sun C-W, Soloway RD, Xu D-F, Wu Q-G, Sun K-H, Weng S-F, Xu G-X (2001) Distinguishing malignant from normal oral tissues using FTIR fiber-optic techniques. *Biopolymers* 62:185–192
29. Shaikh S, Yadav DK, Rawal R (2021) Saliva based non invasive screening of Oral Submucous Fibrosis using ATR-FTIR spectroscopy. *J Pharma Biomed Anal* 203:114202
30. Zlotogorski-Hurvitz A, Dekel BZ, Malonek D, Yahalom R, Vered M (2019) FTIR-based spectrum of salivary exosomes coupled with computational-aided discriminating analysis in the diagnosis of oral cancer. *J Cancer Res Clin Oncol* 145:685–694
31. Banerjee S, Pal M, Chakrabarty J, Petibois C, Paul RR, Giri A, Chatterjee J (2015) Fourier-transform-infrared-spectroscopy based spectral-biomarker selection towards optimum diagnostic differentiation of oral leukoplakia and cancer. *Anal Bioanal Chem* 407:7935–7943
32. Rai V et al (2018) Serum-based diagnostic prediction of oral submucous fibrosis using FTIR spectrometry. *Spectrochim Acta Part A Mol Biomol Spectrosc* 189:322–329

Publisher's Note Springer Nature remains neutral with regard to jurisdictional claims in published maps and institutional affiliations.

Springer Nature or its licensor (e.g. a society or other partner) holds exclusive rights to this article under a publishing agreement with the author(s) or other rightsholder(s); author self-archiving of the accepted manuscript version of this article is solely governed by the terms of such publishing agreement and applicable law.